

Article

A Comparative Case Study on Drainage Consolidation Improvement of Soft Soil under Vacuum Preloading and Surcharge Preloading

Ling Fan, Zhize Xun and Shuquan Peng * 

School of Resources and Safety Engineering, Central South University, Changsha 410083, China; pqrfanlinger@csu.edu.cn (L.F.); xunzhize@csu.edu.cn (Z.X.)

* Correspondence: pqr97linger@csu.edu.cn

Abstract: Based on an improvement project of soft soil ground in Zhuhai City on the Pearl River Delta, a comparative study on vacuum preloading and surcharge preloading was performed. The ground and stratified settlements, excess pore water pressure, and the degrees of consolidation of soft soil are analyzed, along with the horizontal displacement and soil strength. The results show that surcharge preloading results in smaller secondary consolidation settlements than vacuum preloading. Primary consolidation settlement quickly increases with increasing excess pore water pressure of less than -40 kPa in vacuum preloading, while also increasing between 20 kPa and 25 kPa in surcharge preloading. The sharp increase in the strata permeability coefficient will induce the increase in strata consolidation degree and has little effect on the ground consolidation degree. The surcharge preloading can be given priority to reduce the settlement foundation in the service stage.

Keywords: vacuum preloading; surcharge preloading; consolidation degree; settlement; excess pore water pressure



Citation: Fan, L.; Xun, Z.; Peng, S. A Comparative Case Study on Drainage Consolidation Improvement of Soft Soil under Vacuum Preloading and Surcharge Preloading. *Appl. Sci.* **2023**, *13*, 5782. <https://doi.org/10.3390/app13095782>

Academic Editor: Zhen-Dong Cui

Received: 11 April 2023

Revised: 30 April 2023

Accepted: 3 May 2023

Published: 8 May 2023



Copyright: © 2023 by the authors. Licensee MDPI, Basel, Switzerland. This article is an open access article distributed under the terms and conditions of the Creative Commons Attribution (CC BY) license (<https://creativecommons.org/licenses/by/4.0/>).

1. Introduction

Soft soil is widely distributed close to lakes and the middle and lower reaches of rivers all over the world. The Pearl River Delta, located on the southeast coast of China, serves as one example of such an area. The physical and mechanical properties of soft soils are highly intricate, characterized by low strength, high moisture content, high compressibility, and high sensitivity to external disturbances [1]. Improper treatment of the soft soil base can result in a range of practical engineering issues, including uneven ground settlement and large post-work settlement over a longer period. These issues can impact the structural stability and long-term safety of various buildings constructed on such soil [2,3]. Hence, it is imperative to improve soft soil conditions before utilizing it as a foundation for any building. Vacuum preloading, surcharge preloading, and combined preloading are commonly used practical methods to enhance soft soil conditions [4–8].

Figure 1 illustrates the schematics of vacuum preloading and surcharge preloading methods. These methods aim to drain the pore water from the ground through a pre-loaded vertical and horizontal drainage system, and as the pore water dissipates, the pore volume of the soil then decreases, consolidation and settlement of the foundation occurs, and the effective stress and strength of the foundation soil gradually increases. The drainage consolidation models of the ground by preloading are presented [9–13].

Some innovations are provided to improve the vacuum preloading method. For example, the expansion of dissolved gas in water, thermal preloading, and prefabricated boosters are used to accelerate water drainage [6,7,14,15]. The optimal surcharge preloading rate minimizes the lateral displacement [16], and the sealing membrane with clay reduces the total cost by replacement [17].

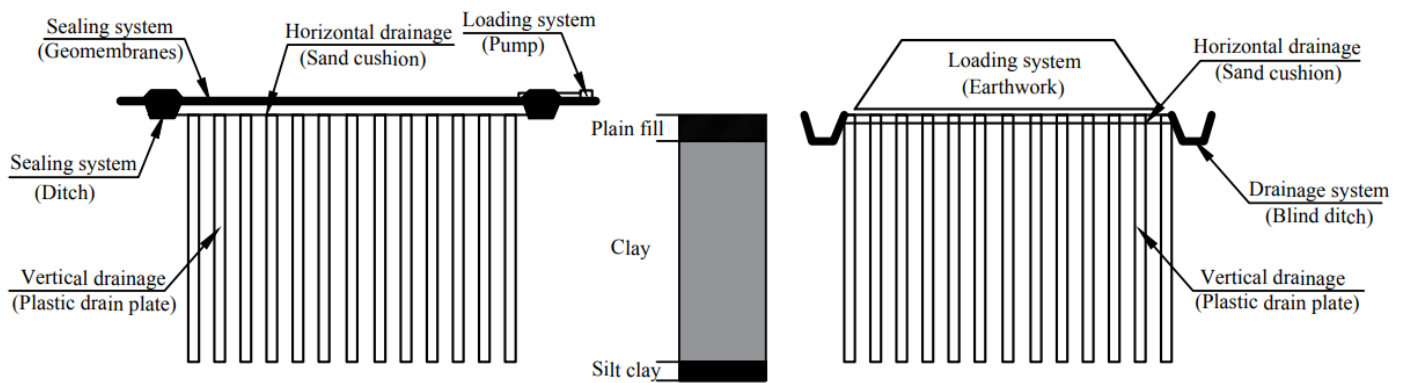


Figure 1. Schematic diagram of vacuum and surcharge preloading method.

Some case studies have shown that vacuum preloading resulted in more consolidation degree and less consolidation settlement than surcharge preloading [18–21]. The consolidation settlement is composed of immediate, primary, and secondary consolidation settlements [5,22]. The immediate and primary consolidation settlements of the ground are mostly completed during the preloading stage. However, during the service stage, when the ground is used as a foundation for buildings, secondary consolidation settlements continue to occur due to soft soil creep under the additional stress. The uneven secondary consolidation settlement in the service stage will reduce the safety of the building on the ground and will even destroy the building. Therefore, it is necessary to investigate the impact of vacuum and surcharge preloading on the immediate, primary, and secondary consolidation settlement of ground to minimize the detrimental effects of uneven secondary consolidation settlement on the building [19,23]. However, such effects have not been thoroughly studied.

This study outlines an improvement project for soft soil ground in Zhuhai City and conducts a case comparative study to investigate the diversity of primary and secondary consolidation settlement resulting from ground improvement by vacuum preloading and surcharge preloading, including the effects of excess pore water pressure, horizontal displacement, and soil strength.

2. Site Condition

This improvement project is located in Zhuhai City, Guangdong Province, between Heyi East Road and Heyi West Road. This project has an L-shaped site with a total area of 128,000 m² and is divided into a vacuum preloading region and a surcharged preloading region with an area of 53,000 m² and 75,000 m², respectively, as depicted in Figure 2. Table 1 tabulates the profile of the strata and the mechanical parameters of each soil stratum at the site. The table reveals that the site is primarily composed of a soft soil stratum, which has a thickness of 19.24 m below ground level, as determined by geotechnical investigation. The layout of exploratory holes from the geotechnical investigation is illustrated in Figure 2. The groundwater table is situated at a depth of 1.37 m from ground level.

Table 1. Parameters of soil strata.

Soil Strata	Unit Weight of Natural (γ) (N·m ⁻³)	Elastic Modulus (Es) (MPa)	Natural Water Content (W) (%)	Soil Cohesion (c) (kPa)	Compression Factor (a_{1-2}) (MPa ⁻¹)	Horizontal Permeability (k_h) (cm·s ⁻¹)	Friction Angle (ϕ) (°)	Void Ratio (e) (-)	Stratum Thickness (h) (m)	Pile Friction Resistance (kPa)
Plain fill	18.0	3.89	38.2	5.0	1.876	8.11×10^{-7}	5.00	0.801	3.14	15
Clay	15.2	1.76	73.6	2.9	1.138	9.81×10^{-8}	2.30	2.513	19.24	11
Silt clay	17.3	3.40	48.1	8.3	1.142	2.31×10^{-7}	9.10	1.571	3.93	30

Notes: ϕ is friction angle, and the results are from direct shear tests.

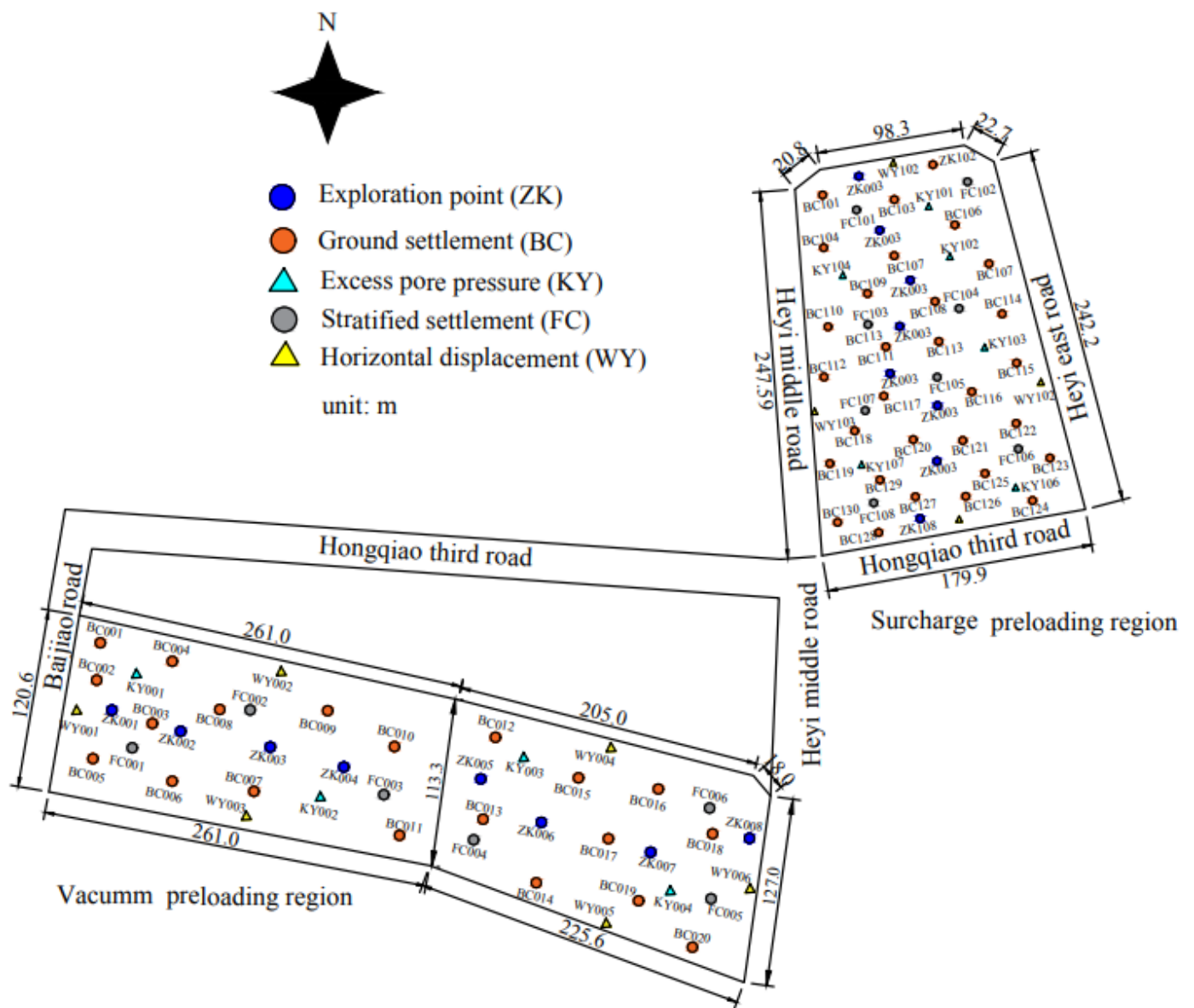


Figure 2. Schematic of the field test.

3. Construction Processes

Before the implementation of improvements, the length of the PVDs and the total pressures of surcharge preloading and vacuum preloading were fixed at 21.0 m and 80 kPa, respectively. According to the Code for Foundation Treatment, the PVDs were a cross-section of 100 mm × 4 mm with an equivalent diameter of 66 mm, and they were designed to be installed in a triangular pattern at a spacing of 1.2 m in the two improving regions. Secondly, a 0.5 m thick sand cushion was laid on the two regions. In the vacuum preloading region, the vertical draining pipe, vacuum pump, horizontal draining pipe, sealing membrane (geo-members), and sealing ditch were successively installed by on-scene operation. The vacuum pump was then started, and the vacuum pressure under the membranes achieved −80 kPa on the 20th day, and this was maintained for 63 days. The total period of vacuum preloading was 83 days, and in the surcharge preloading region, the water collection well, sealing membrane, blind ditch, and surcharge load were also successively applied by on-scene operation. The surcharge load material was selected to be clay soil with a unit weight of 17.8 kN/m³, and the surcharge fill was constructed up to 4.5 m height with an equivalent pressure of 80.1 kPa in 30 days, which then lasted for 53 days.

During the total period of vacuum preloading and surcharge preloading, various parameters were monitored in the two regions targeted for improvement, including ground settlement, stratified settlement, horizontal displacement, and excess pore water pressure. The number and sequence of monitoring points and holes are tabulated in Table 2, and the layout of monitoring points and holes is plotted in Figure 2. In order to monitor the settlement amount and settlement process of each soil layer and to grasp the deformation of each soil layer under vacuum, ground vertical settlement and horizontal displacement were monitored using a LeicaNA730 balance level with an accuracy of 1.2 mm/km and a LeicaTZ08 total station with an accuracy of 1 s, respectively. In order to monitor the settlement amount and settlement process of each soil layer and to grasp the deformation of each soil layer under vacuum pre-pressure and mound pre-pressure, eight CJY-7090 high-precision stratified settlement gauges with a measurement accuracy of 1 mm were fixed at intervals of 3.0 m in a 24 m stratified settlement tube, respectively, and the stratified settlement of the soil was obtained by monitoring the synchronous sinking amount of the magnetic settlement ring fixed on the settlement tube with the settlement of the foundation. It is worth mentioning that the accuracy of the measurement results is greatly influenced by the selection of the reference point, and it is necessary to ensure that the settlement tube enters the soil-bearing layer, otherwise, the compression and settlement of the soil at the bottom of the tube produces relatively large measurement errors.

Table 2. Monitoring points for vacuum preloading and surcharge preloading.

Monitoring Items	Vacuum Preloading		Surcharge Preloading	
	Number	Sequence	Number	Sequence
Ground settlement	20	BC001-BC020	30	BC101-BC130
Excess pore water pressure	4	KY001-KY004	6	KY101-KY106
Stratified settlement	6	FC001-FC006	8	FC101-FC108
Horizontal displacement	6	WY001-WY006	4	WY101-WY104

The pore water pressure was monitored using a KXR-3030 vibrating wire pore water pressure transducer, buried at the monitoring location in a one-hole multi-point pattern. The KXR-3030 vibrating wire pore water pressure transducer has a resolving power of $\leq 0.08\%$ F.S (Full scale) and a combined error of $\leq 1.5\%$ F.S. It mainly consists of a probe, a frequency reading instrument, and a cable, which translates the change in pore water pressure by measuring the frequency change of the internal steel string. Seven vibrating wire pore water pressure transducers were buried at 3.0 m intervals in each excess pore water pressure hole from a depth of 3 m to 21 m.

The shear strength of the soil is related to the stability of the foundation, and the direct shear test is a common method to determine the shear strength of the soil, with the advantages of simple operation and high-test efficiency. The static load test is currently one of the most intuitive and reliable testing methods to determine the bearing capacity [24–26]. Most foundations should be tested for bearing capacity using static load tests. In this case, after improvement, soil strength and pile friction resistance of improved soil was presented by direct shear test and field static load test, respectively.

4. Calculation of Primary and Secondary Settlement

Based on the mechanics of soil consolidation, the ground settlement is composed of instant settlement (S_i), primary consolidation settlement (S_p), and secondary consolidation settlement (S_s) caused by creep. Therefore, the final settlement by the consolidation method is presented. The final settlements (S_∞) of two improved regions are also analyzed by the consolidation model method proposed by:

$$S_\infty = S_i + S_p + S_s, S_t = S_i + S_{pt} + S_{st} \quad (1)$$

where S_t is average ground and strata consolidation settlement at time of t , and S_{pt} and S_{st} are the primary consolidation settlement and secondary consolidation settlement caused by creep at time t .

During the primary consolidation settlement stage, S_{st} is very small and is therefore ignored. Then:

$$S_{pt} = S_t - S_i \tag{2}$$

The primary consolidation settlement and its rate are written as:

$$S_{pt} = \bar{U}_t S_p, \dot{S}_{pt} = \dot{\bar{U}}_t S_p \tag{3}$$

where S_{pt} and \dot{S}_{pt} are the primary consolidation settlement and its rate, respectively. \bar{U}_t is the average of consolidation degree by $\bar{U}_t = \sum_{i=1}^1 \frac{q_i}{\sum \Delta p} [(T_i - T_{i-1}) - \frac{\alpha}{\beta} e^{-\beta T_i} (e^{\beta T_i} - e^{\beta T_{i-1}})]$, where q_1 is the loading rate of 80/20 and 80/30 kPa/d for vacuum and surcharging preloading, respectively; $\sum \Delta p$ is the cumulative loads (80 kPa); and T_1 and T_0 are the start time and end time for load No.1, respectively. When the conditions of vertical and inward radial drainage are applied, $\alpha = \frac{8}{\pi^2}$, $\beta = \frac{8}{F(n)} \frac{C_h}{d_c^2} + \frac{\pi^2}{4} \frac{C_v}{H^2}$, where $n = d_e/d_w = 19.09$, $n = F(n) = \frac{n^2}{n^2-1} \ln n - \frac{3n^2-1}{4n^2}$. C_h and C_v are the horizontal and vertical consolidation coefficients (cm²/s), respectively. $C_v = k(1+e)/a_{1-2}\gamma_w$, where k, e, a_{1-2} and γ_w are listed in Table 1. In the paper, $C_h = C_v$.

Substituting \bar{U}_t in Equation (3), the following can be obtained:

$$\dot{S}_{pt} + \beta S_{pt} = \sum_{i=1}^1 \frac{q_i}{\sum \Delta p} (T_i - T_{i-1}) S_p \tag{4}$$

Equation (4) is the first order differential equation of S_{pt} , proposed by Asaoka [27]. Then, substituting S_{pt} in Equation (4) with Equation (2), the following is obtained:

$$\dot{S}_t + \beta S_t = \sum_{i=1}^1 \frac{q_i}{\sum \Delta p} (T_i - T_{i-1}) S_p + \beta S_i \tag{5}$$

Equation (5) shows that the average ground settlement rates (\dot{S}_t) is liner to the S_t with the slope ($-\beta$) and intercept (b_c) fitted by least square method.

Where $\dot{S}_t = 0$, S_t is the sum of S_p and S_i , and is denoted as S_{pi} . S_{pi} is calculated by:

$$S_{pi} = \frac{b_c}{\beta} = S_p + S_i \tag{6}$$

and based on the measured settlement, \bar{U}_t is also rewritten as:

$$\bar{U}_t = \frac{S_{pt}}{S_p} = \frac{S_t - S_i}{S_{pi} - S_i} \tag{7}$$

so S_i was deduced and calculated by:

$$S_i = \frac{S_t - \bar{U}_t S_{pi}}{1 - \bar{U}_t} \tag{8}$$

Then, S_p is presented by:

$$S_p = S_{pi} - S_i \tag{9}$$

During the secondary consolidation settlement stage, the increment of S_{pt} is very small and keeps a constant of S_p , then:

$$S_{st} = S_t - S_i - S_p \tag{10}$$

The S_{st} is analyzed by the Voigt–Kelvin model [23], and is presented by:

$$E_v S_{st} + K_e \dot{S}_{st} = p H \tag{11}$$

where \dot{S}_{st} is the secondary settlement rate; E_v and K_e is the elastic model of spring and viscosity coefficient of Newton dashpot in the Voigt–Kelvin model; and p is loading on the ground.

So, during the secondary consolidation stage, the relationship between consolidation settlement rate and the consolidation settlement is also a line with the slope ($-\beta_s$) and intercept (b_s), and β_s and b_s are fitted by the least square method. The final consolidation settlement is presented by:

$$S_\infty = \frac{b_s}{\beta_s} \tag{12}$$

$$S_s = S_\infty - S_i - S_p \tag{13}$$

Equation (11) is solved by:

$$S_{st} = \frac{p H}{E_v} \left(1 - e^{-\frac{E_v}{K_e} t} \right) \tag{14}$$

So $t \rightarrow \infty$, $E_v = p H / S_s$. When $t = 83$ d, $S_{st} = S_{83} - S_i - S_p$.

5. Results and Discussions

5.1. Measured Settlements

Figure 3 and Table 3 show the ground settlements (S_{gs}) and the stratified settlements (S_{ss}) in the vacuum and surcharge preloading regions. As shown in Figure 3 and Table 3, on the 83rd day, the central S_{gs} and S_{83} in the vacuum preloading region are 0.7 to 0.93 times that in the surcharge preloading region.

Table 3. Consolidation degrees using ground and stratified settlements of vacuum preloading and surcharge preloading.

Depth/m	Vacuum Preloading			Surcharge Preloading		
	S_{83}/mm	S_∞/mm	S_{83}/S_∞	S_{83}/mm	S_∞/mm	S_{83}/S_∞
0	1098	1204	91%	1185	1317	90%
3	820	898	91%	999	1105	90%
9	660	734	90%	815	911	89%
15	350	413	85%	500	565	88%
21	75	83	90%	88	93	95%

These ratios belong in the range from 0.8 to 1.0 provided by Chai [28]. Figure 3 also shows that S_{ss} reduce along depth and have a good fitness by negative exponential function with correlation coefficients of 0.93 and 0.87, respectively.

The consolidation degree, U_{st} , is calculated by the ratio of S_t to the final average settlements of ground and strata ($S_{1,\infty}$), predicted by the hyperbolic method with the formulas $S_t = S_0 + \frac{t}{\alpha_1 + \beta_1 t}$ and $S_{1,\infty} = S_0 + \frac{1}{\beta_1} (t \rightarrow \infty)$. S_0 is the measured ground and stratified settlement (mm) on the 20th day and 30th day for vacuum and surcharge preloading with 80 kPa, respectively; α_1 and β_1 are constants. $S_{1,\infty}$ and U_{st} are tabulated in Table 3. Table 3 shows that U_{st} of foundation depth from 0 m to 15 m by the vacuum preloading is 1% greater than the one of surcharge preloading, while the U_{st} of vacuum at a depth of 15–21 m is 3% to 5% smaller than the one of surcharge.

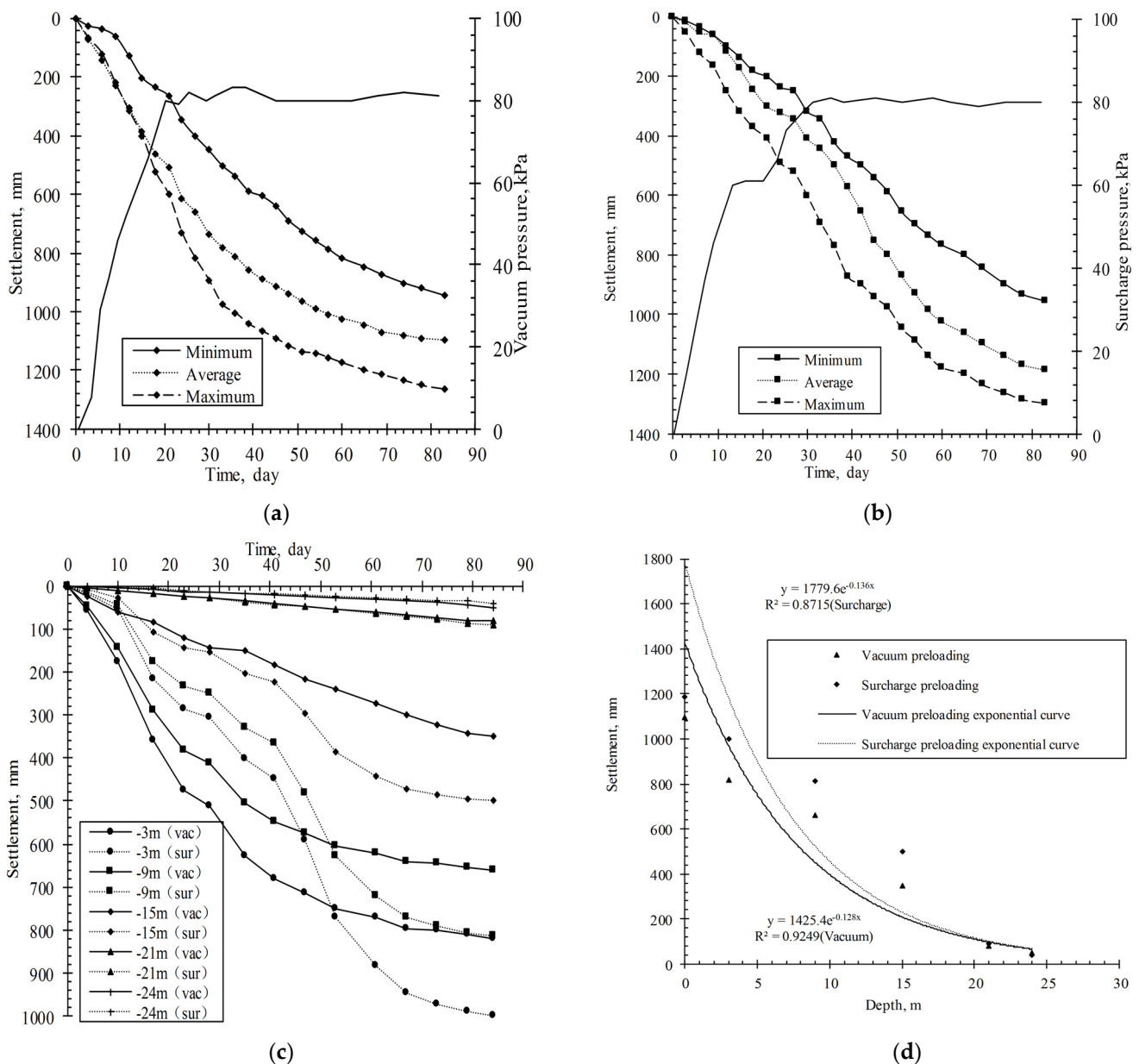


Figure 3. Curves of ground settlements and stratified settlements: (a) historical curve of ground settlements in the vacuum preloading; (b) historical curve of ground settlements in the surcharge preloading; (c) historical curve of stratified settlements; (d) fitting function of stratified settlements.

Figure 3c shows the curves of the stratified settlements. In contrast to surcharge preloading, vacuum preloading reinforcement of soft foundations exhibits an accelerated increase in soil strength during the initial stages, followed by a deceleration in the later stages of reinforcement. Conversely, surcharge preloading demonstrates a more gradual increase in soil strength throughout the reinforcement process [29]. This distinction is attributed to the disparate reinforcement mechanisms inherent to each preloading method.

Vacuum preloading employs an impermeable plastic film and geotextile sealing to strengthen soft ground foundations. By generating negative pressure within the soil, vacuum pumps facilitate the gradual extraction of soil pore water and air, leading to a continuous decrease in pore water pressure and an increase in the foundation’s effective stress. The vacuum pressure’s direct action on the fluid within the soil pores and indirect action on the soil skeleton via the pore fluid approximates an isotropic isobaric situation, enabling

immediate application of the set load value. Consequently, a larger initial settlement is attained, and ground settlement remains relatively uniform [22,30].

In contrast, surcharge preloading applies the external load directly to the soil skeleton or particles, necessitating a stepwise loading process that precludes a one-time application of the set load value. Moreover, trapped air bubbles within the soil cannot be discharged during the extrusion process, potentially obstructing the pores and reducing soil permeability. This effect decelerates the consolidation process, resulting in a consolidation rate inferior to that of vacuum preloading.

5.2. Primary and Secondary Settlement Analysis

Figure 4 illustrates the correlation between \dot{S}_t and S_t for both vacuum preloading and surcharge preloading. Using the slopes and intercepts of the \dot{S}_t - S_t curve in Figure 4 and Equations (8), (9), (12), and (13), S_{∞} , S_i , S_p , and S_s are calculated and tabulated in Table 4. Then, E_s , E_v , and K_e are calculated as 4.19 MPa, 6.83 MPa, and 4726.80 MPa/d in the surcharge preloading region, while they are 4.48 MPa, 4.67 MPa, and 3433.90 MPa/d in the vacuum preloading region.

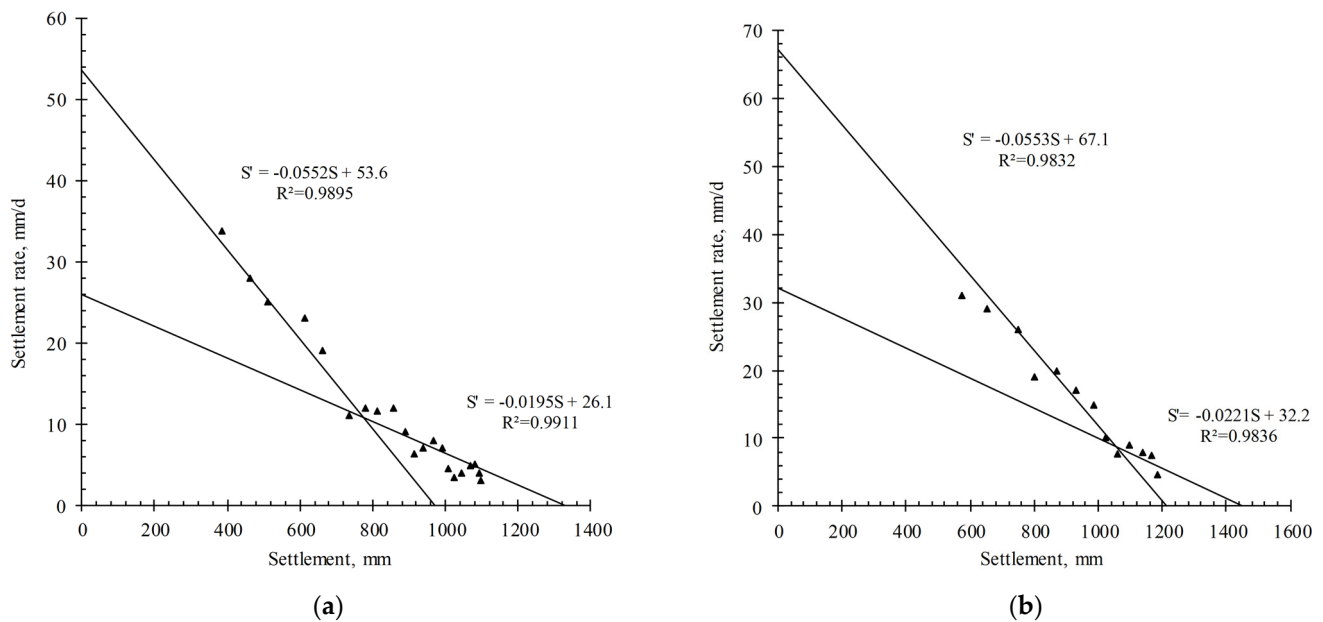


Figure 4. Curves of settlement rate and settlement: (a) vacuum preloading; (b) surcharge preloading.

Table 4. Ground settlements by consolidation model method.

	Vacuum Preloading		Surcharge Preloading	
	Settlement	Settlement Ratio	Settlement	Settlement Ratio
immediate	375.4	28.2%	400.2	26.7%
primary consolidation	594.6	44.7%	804.8	55.5%
secondary consolidation	360	27.1%	246	17.0%
final	1330	100%	1451	100%

Table 4 shows that the instant settlement, S_i , the primary consolidation settlement, S_p and the secondary consolidation settlement, S_s , of vacuum preloading account for 28.2%, 44.7%, and 27.1% of the final settlements, S_{∞} , while the ones of surcharged loading do 26.7%, 55.5%, and 17.0% of S_{∞} . This means that the S_s/S_{∞} during vacuum preloading is 1.6 times that during surcharge preloading. The reason for this is speculated as follows: Firstly, in Section 5.1 on the 83rd day, the U_{st} of vacuum preloading is less than the one of surcharge preloading. In other words, $S_s/S_{\infty} = 1 - U_{st}(t = 83)$ of the vacuum preloading is greater than the one of the surcharge preloading. Secondly, the surcharge preloaded

foundation undergoes an additional stress field by a similar loading method for preloading and service stage, while the vacuum preloaded one is subjected to a negative pressure seepage field in the preloading stage and to an additional stress field in the service stage.

Figure 5 depicts the predicted curves for S_i , S_{pt} , and S_{st} plotted against time. From Figure 5 it can be deduced that after preloading, S_i and S_{pt} tend to stabilize within 83 days, while S_{st} is smaller. In the service after the 83rd day, the S_{gs} is still increasing for a long time of 10 ten years and is dominated by S_{st} . If the S_{st} of the preloading improved ground is over excessive, this may result in adverse settlement and settlement differences during the life of the building, reducing the serviceability of the foundations.

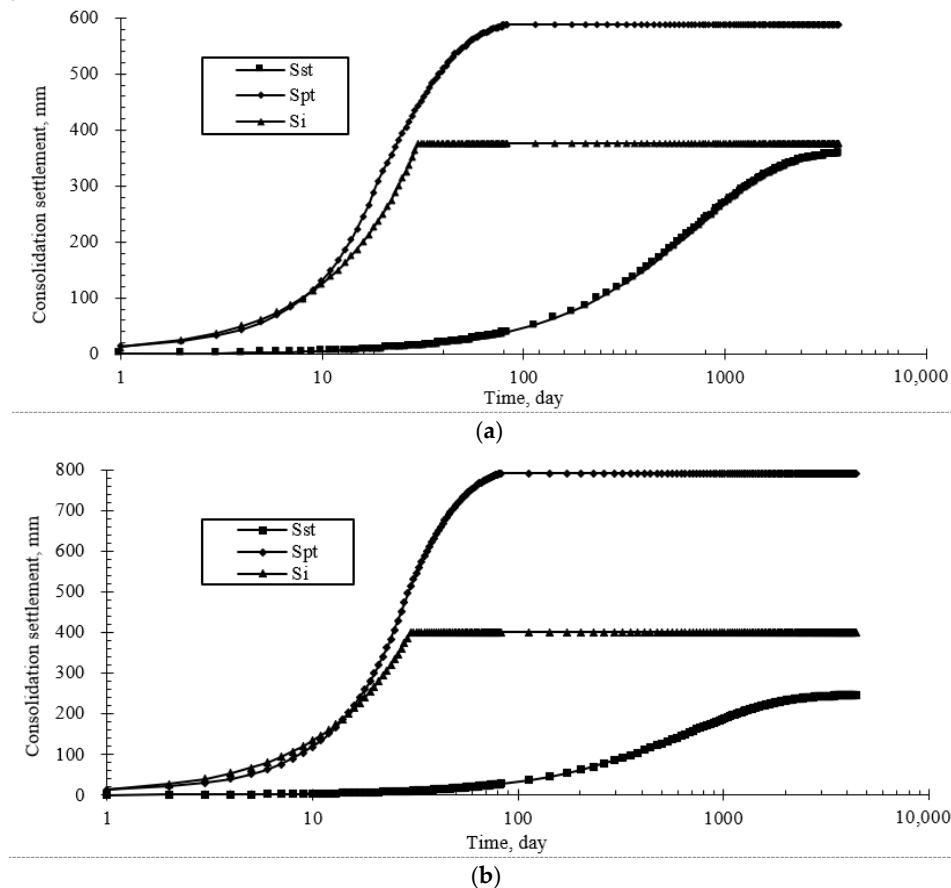


Figure 5. Predicted curve of S_i , S_p , and S_s using S_{gs} vs. time: (a) vacuum preloading; (b) surcharge preloading.

During the primary consolidation phase, soil consolidation primarily arises from the expulsion of air and free water within the pores. Conversely, secondary consolidation chiefly occurs due to the reorganization of soil grain structure and the creep of bound water films on soil grain surfaces. As illustrated in Figure 5, the duration required for vacuum preloading consolidation to achieve settlement stability is notably longer compared to surcharge preloading consolidation. The reason for this may be that the vacuum preloading method acts on the pore water vapor fluid in the soil, and as pore water and gas dissipate, the pore space between soil particles gradually expands, inducing the rearrangement and compaction of soil particles without incurring shear damage or particle breakage. In contrast, the external load of surcharge preloading is applied directly to the soil skeleton or particles. The compression or disintegration of the skeleton prompts the translation or rotation of clay agglomerates, culminating in the internal cementation fracture of these agglomerates. Macroscopically, this process manifests as creep deformation of the soil. However, due to the rearrangement and fragmentation filling of soil particles, the soil becomes more compact and exhibits enhanced settlement consolidation [19,22,30].

Therefore, the surcharge preloading has priority compared with vacuum preloading in reducing the ground settlement of ground during its service.

5.3. Relationship between Excess Pore Water Pressures and Primary Consolidation Settlement

Figure 6 plots the average excess pore water pressures (u_t). As shown in Figure 6, the u_t monotonously increases up to the maximums on the 63rd day, then basically remains stable in vacuum preloading. On the 63rd day, the u_t of vacuum preloading decays linearly from -70 kPa to -10 kPa along the depth of the ground, with an attenuation coefficient of 3.1 kPa/m. The reason for this is the PVDs's block, bending, and brakeage induced by stratified settlement [6,9,17,31–34]. The u_t of surcharge preloading reaches maximum on the 30th day, then dissipates up to the minimums on the 53rd day. The u_t of surcharge preloading on the 30th day is piecewise linear along depth, i.e., it increases from 15 kPa to 30 kPa with depth in the range of 3 – 15 m, and slightly reduces to 27 kPa with depth in the range of 15 – 21 m. The u_t monotonously increases up to the maximum on the 63rd day, then basically remains stable in vacuum preloading. This shows existents in soil structure compression and stress redistribution during the consolidation process [5].

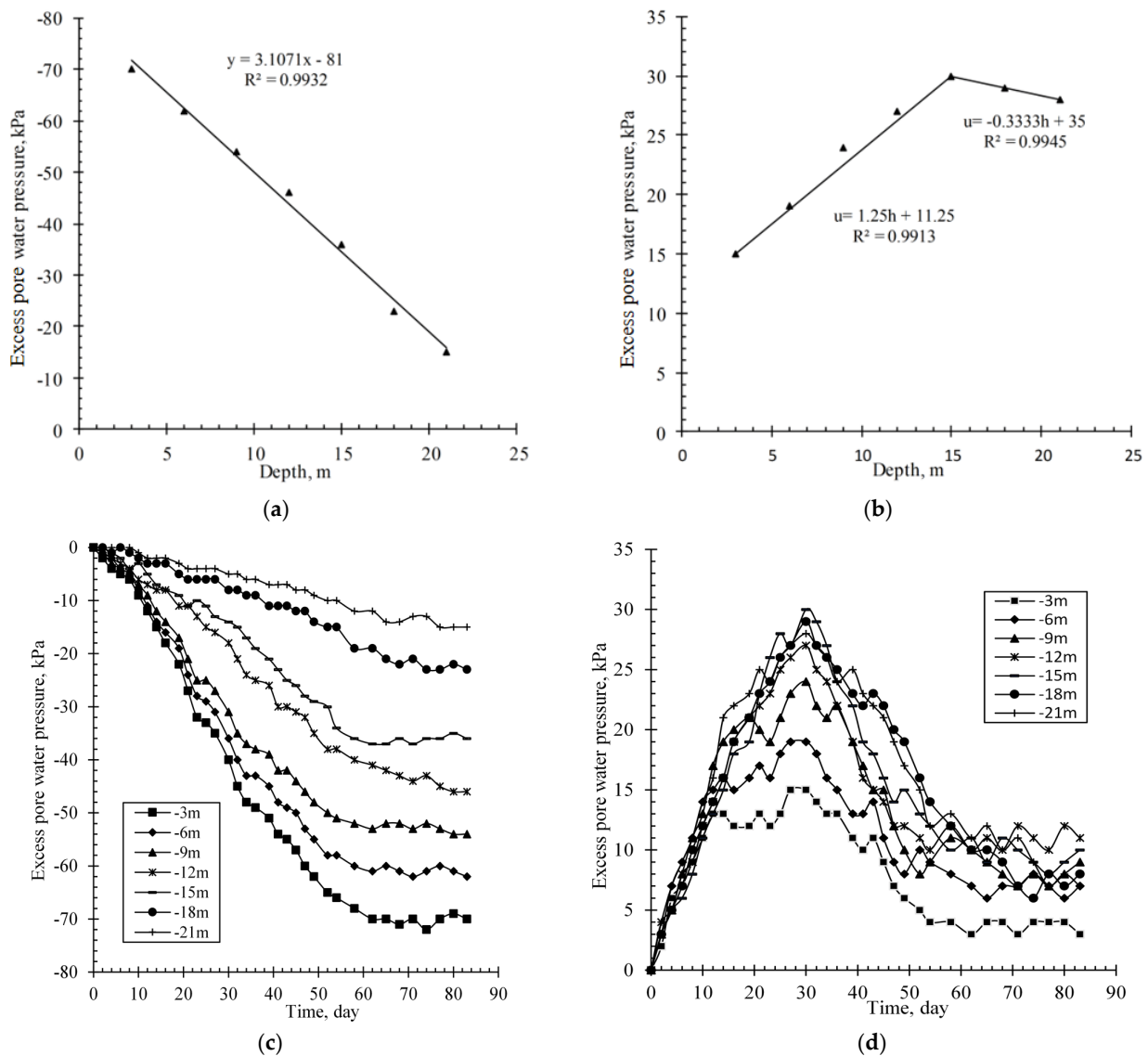


Figure 6. u_t of vacuum preloading and surcharge preloading: (a) distribution of u_t along the depth of vacuum preloading; (b) distribution of u_t along the depth of surcharge preloading; (c) historical curve of vacuum preloading; (d) historical curve of surcharge preloading.

The consolidation degrees (U_{wt}) are plotted in Figure 6 and tabulated in Table 5. U_{wt} is calculated using u_t by the hyperbolic method with the formula $u_t = u_0 + t/(\alpha_2 + \beta_2 t)$, $u_\infty = u_0 + \frac{1}{\beta_2}(t \rightarrow \infty)$, $U_{wt} = \frac{\Delta u_t}{\Delta u_\infty}$, where u_0 refers to the measured average excess pore water pressure (kPa) at any depth on the 20th day and 30th day in vacuum and surcharge preloading, respectively. Δu_t is the difference between u_t and its maximum (kPa). u_∞ is the final excess pore water pressure. α_2 and β_2 are the constants. As shown in Table 5, the U_{wt} decreases with the depth from 3 m to 15 m, then increases from 15 to 21 m on the 83rd day.

Table 5. Stress consolidations degree of vacuum preloading and surcharge preloading.

Depth/m	Vacuum Preloading				Surcharge Preloading			
	β_2	$\Delta u_{83}/\text{kPa}$	$\Delta u_\infty/\text{kPa}$	$\Delta u_{83}/\Delta u_\infty$	β_2	$\Delta u_{83}/\text{kPa}$	$\Delta u_\infty/\text{kPa}$	$\Delta u_{83}/\Delta u_\infty$
3	0.0193	45	52	87%	0.0711	12	14	85%
9	0.0232	36	43	84%	0.0543	15	18	83%
15	0.0301	26	33	78%	0.0394	20	25	79%
21	0.0761	11	13	82%	0.0386	21	26	81%

Figure 7 plots the primary consolidation settlement (S_{pt}) vs. u_t . The secondary consolidation settlement (S_{st}) during preloading retains a low level, and the effect of u_t on S_{st} can be ignored. Figure 7a shows that during the vacuum preloading, the S_{pt} obviously increases by 540 mm, equal to 90% primary consolidation settlement, with u_t ranging from 0 kPa to -40 kPa, while it gently increases by approximately 60 mm with u_t over -40 kPa. Therefore, it can be deduced that u_t with -40 kPa is an important value during the monitoring of u_t , S_t in the vacuum preloading. As shown in Figure 7b, during the surcharge preloading, S_{pt} slowly increases with u_t beneath 20 kPa and increases significantly with u_t between 20 kPa and 25 kPa.

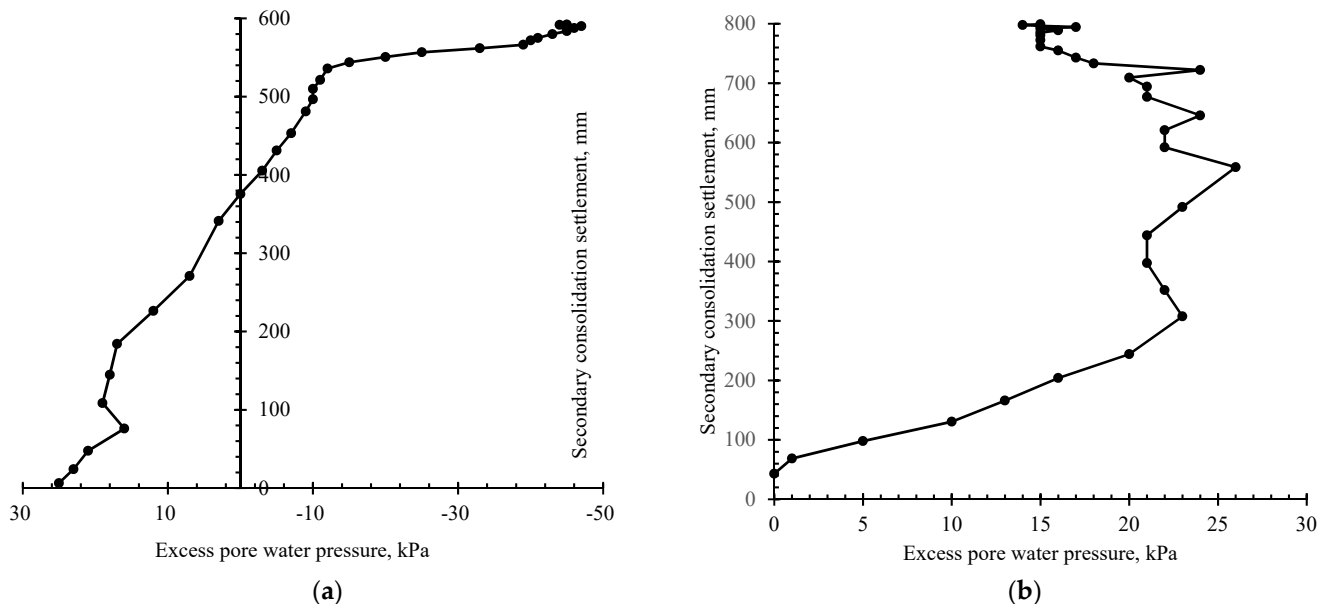


Figure 7. The S_{pt} and u_t at a depth of 15 m: (a) vacuum preloading; (b) surcharge preloading.

5.4. Horizontal Displacement and Soil Strength and Effects on Primary Consolidation Settlement

Figure 8 plots the horizontal displacement. Figure 8 shows that horizontal displacement induced by vacuum preloading with a maximum of 263 mm (point WY104) moving toward the center is 1.2 times the one by surcharge preloading, with a maximum of 218 mm

(point WY002) moving in the negative direction. Because of the horizontal displacement and S_{pt} increase with the time, it can be presumed that S_{pt} grows with the increase in horizontal displacement [35].

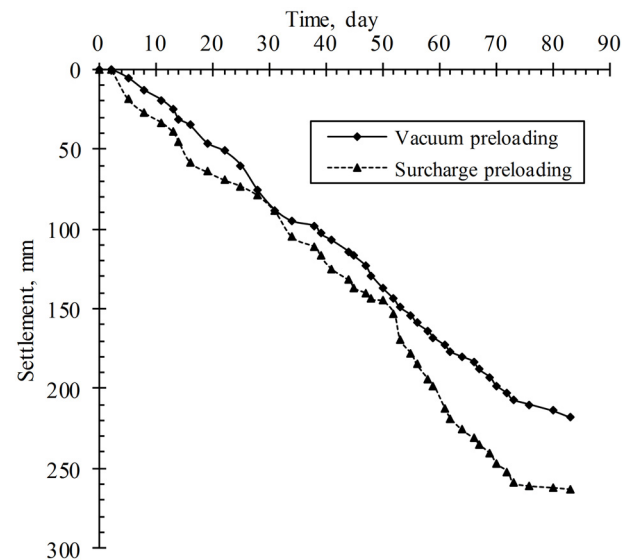


Figure 8. Historical curve of horizontal settlement.

After vacuum and surcharge preloading, the cohesion (c) and internal friction angle (φ) of clays increase from 2.9 kPa to 4.3~4.4 kPa and from 2.30° to 2.92~2.99°, respectively, and the pile side friction resistance increases from 7.0 kPa to 10.2~11.3 kPa.

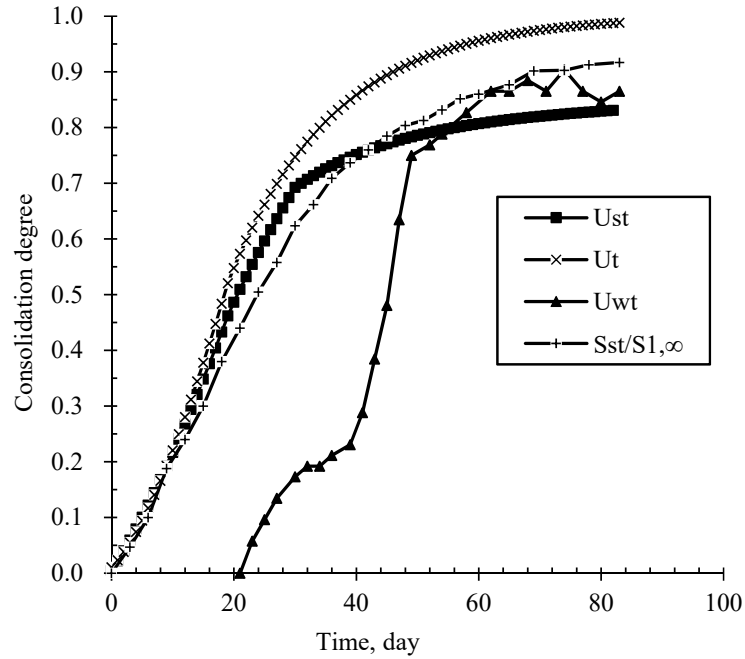
With the application of vacuum preloading, cohesion, friction angle, and pile lateral frictional resistance experienced an increase of 48%, 27%, and 46%, respectively. Furthermore, when surcharge preloading pressure was applied, the improvements in cohesion, friction angle, and pile lateral frictional resistance were observed to be 52%, 31%, and 61%, respectively. Similarly, the deformation parameters such as E_s , E_v , and K_e were also improved, and the increasing of E_s , E_v , and K_e reduce the S_{pt} and S_{st} . These findings underscore the efficacy of both vacuum preloading and the application of additional preloading pressure in bolstering the soil's mechanical properties and overall performance; the results indicate a substantial enhancement of soft soil ground properties in the improvement project.

5.5. Discussions

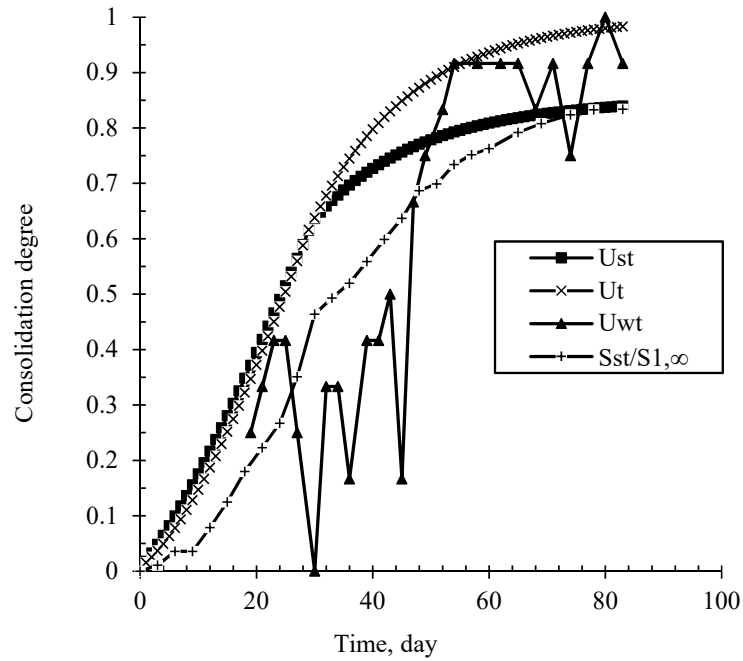
The measured ground settlement difference for vacuum preloading is smaller than that of surcharge preloading. This may be because the vacuum preloading applies a relatively more uniform pressure on the ground than surcharge preloading, which initializes the trapezoid pressure with small value at the sides and a large one in the center. This is verified by Zhang et al. [19]. Therefore, the vacuum preloading benefits to reduce differential ground settlement [20,36,37].

As can also be seen from Figure 3c, the stratified settlements at the depth of 21 m are less than 100 mm, approximately 7% of the ground settlements, in the vacuum and surcharge preloading. Therefore, the depth of 21 m can be regarded as the influence depth of vacuum preloading and surcharge preloading. Figure 6 shows that the U_{st} decreases as depth increases, while there are increases at the depth of 21 m in the two preloading regions. This may be because the permeability of soil (k) and the void ratio (e) of this site decreases with increasing depth, while sharply increasing at a depth of approximately 21 m close to the stratigraphic boundary between clay and silt clay (seen Table 1) [34,36,38]. The sharp increasing of strata permeability coefficient will induce the increase in strata U_{st} and has little effect on the ground U_{st} .

The consolidation degrees denoted as \bar{U}_t , U_{st} , U_{wt} , calculated by the consolidation model method [39], S_t and u_t for vacuum and surcharging preloading, respectively, are plotted in Figure 9. Figure 9 shows that in vacuum and surcharging preloading, the \bar{U}_t , U_{st} are close to each other within 35 days after preloading, while they deviate significantly after the 35th day. On the 83rd day, the sequence of consolidation degree from the maximum to the minimum is \bar{U}_t , U_{st} , U_{wt} . The U_{wt} is less than U_{st} within 50 days and is relatively close to U_{st} after the 50th day.



(a)



(b)

Figure 9. The consolidation degrees denoted as \bar{U}_t , U_{st} , U_{wt} and $\frac{S_{st}}{S_{1,\infty}}$: (a) vacuum preloading; (b) surcharge preloading.

Based on the definition of \bar{U}_t and U_{st} , the ratio of S_{st} to $S_{1,\infty}$ is calculated by:

$$\frac{S_{st}}{S_{1,\infty}} = U_{st} - \bar{U}_t \frac{S_p}{S_{1,\infty}} - \frac{S_i}{S_{1,\infty}} \quad (15)$$

The S_{st} develops with the increasing of the difference between U_{st} and $\bar{U}_t \frac{S_p}{S_{1,\infty}}$. On the 83rd day, the S_{st} accounts for 9% of $S_{1,\infty}$ in vacuum preloading and 10% in surcharge preloading.

In the drainage consolidation improvement of soft soil, vacuum preloading is more beneficial to reduce the uneven settlement, but in order to reduce the ground settlement of ground during its service, surcharge preloading should be given priority compared with vacuum preloading.

6. Conclusions

Based on the improvement engineering of soft soil ground in Zhuhai City on the Pearl River Delta, a case comparative study on vacuum preloading and surcharge preloading was performed. The conclusions are drawn below:

- (1) Compared to the surcharge preloading method, the vacuum preloading method is more efficient in terms of consolidation time and settlement reduction. However, surcharge preloading results in smaller secondary consolidation settlements than vacuum preloading and should be given priority in order to reduce the settlement foundation in the service stage.
- (2) The primary consolidation settlement (S_{pt}) quickly increases up to 90% of the total primary consolidation settlement (S_p), with an increase in the average excess pore water pressures (u_t) of less than -40 kPa in vacuum preloading, while it also quickly increases, with the average excess pore water pressures (u_t) hovering between 20 kPa and 25 kPa in surcharge preloading.
- (3) The sharp increase in strata permeability coefficient will induce the increase in strata consolidation degrees and has little effect on the ground consolidation degrees.
- (4) The vacuum preloading is more beneficial to reduce uneven settlement, and the surcharge preloading is more beneficial to reduce ground settlement during its service.

Author Contributions: Conceptualization, L.F. and S.P.; methodology, L.F.; software, Z.X.; validation, Z.X.; formal analysis, Z.X.; investigation, L.F.; resources, L.F.; data curation, Z.X.; writing—original draft preparation, Z.X.; writing—review and editing, L.F. and S.P.; visualization, L.F.; supervision, S.P.; project administration, L.F.; funding acquisition, L.F. and S.P. All authors have read and agreed to the published version of the manuscript.

Funding: The research was funded by the National Natural Science Foundation of China (Grant No. 52174100 and No. 51674287), and the National Science Foundation of Hunan Province, China (Grant No. 2021JJ30834).

Institutional Review Board Statement: Not applicable.

Informed Consent Statement: Not applicable.

Data Availability Statement: The data that support the findings of this study are available upon request from the authors.

Acknowledgments: This study was supported by the National Natural Science Foundation of China (Grant No. 52174100 and No. 51674287), and the National Science Foundation of Hunan Province, China (Grant No. 2021JJ30834). We would also like to sincerely thank Guoliang Chen, Kejia Zhang, Jinghong Zheng, and Yuankai Zeng, who gave valuable comments on both the pre-conceptualization and post-revision of the manuscript, which greatly improved the manuscript.

Conflicts of Interest: The authors declare no conflict of interest.

References

1. Lei, H.; Wang, L.; Zhang, W.; Jiang, M.; Bo, Y.; Song, W.; Cao, Q. Geotechnical properties of the South China Sea soft soil: A comparative study with the soils from Bohai Sea and Yellow Sea. *Bull. Eng. Geol. Environ.* **2023**, *82*, 158. [[CrossRef](#)]
2. Indraratna, B. Recent Advances in Vertical Drains and Vacuum Preloading for Soft Ground Stabilisation. In Proceedings of the Proceedings of the 19th International Conference on Soil Mechanics and Geotechnical Engineering, Seoul, Republic of Korea, 17–22 September 2017.
3. Indraratna, B. Recent Advances in the Application of Vertical Drains and Vacuum Preloading in Soft Soil Stabilisation. *Aust. Geomech. J.* **2010**, *45*, 1–44.
4. Kjellman, W. Consolidation of Clayey Soils by Atmospheric Pressure. In *Proceedings of a Conference on Soil Stabilization*; Massachusetts Institute of Technology: Cambridge, MA, USA, 1952; pp. 258–263.
5. Liu, H.-l.; Chu, J. A new type of prefabricated vertical drain with improved properties. *Geotext. Geomembr.* **2009**, *27*, 152–155. [[CrossRef](#)]
6. Artidteang, S.; Bergado, D.T.; Saowapakpi boon, J.; Teerachakulpanich, N.; Kumar, A. Enhancement of efficiency of prefabricated vertical drains using surcharge, vacuum and heat preloading. *Geosynth. Int.* **2011**, *18*, 35–47. [[CrossRef](#)]
7. Wang, J.; Cai, Y.; Ni, J.; Geng, X.; Xu, F. Effect of sand on the vacuum consolidation of dredged slurry. *Mar. Georesour. Geotechnol.* **2018**, *36*, 238–244. [[CrossRef](#)]
8. Indraratna, B.; Rujikiatkamjorn, C.; Ameratunga, J.; Boyle, P. Performance and prediction of vacuum combined surcharge consolidation at Port of Brisbane. *J. Geotech. Geoenviron. Eng.* **2011**, *137*, 1009–1018. [[CrossRef](#)]
9. Cascone, E.; Biondi, G. A case study on soil settlements induced by preloading and vertical drains. *Geotext. Geomembr.* **2013**, *38*, 51–67. [[CrossRef](#)]
10. Mohamedelhassan, E.; Shang, J. Vacuum and surcharge combined one-dimensional consolidation of clay soils. *Can. Geotech. J.* **2002**, *39*, 1126–1138. [[CrossRef](#)]
11. Chai, J.C.; Carter, J.P.; Hayashi, S. Vacuum consolidation and its combination with embankment loading. *Can. Geotech. J.* **2006**, *43*, 985–996. [[CrossRef](#)]
12. Perera, D.; Indraratna, B.; Leroueil, S.; Rujikiatkamjorn, C.; Kelly, R. Analytical model for vacuum consolidation incorporating soil disturbance caused by mandrel-driven drains. *Can. Geotech. J.* **2017**, *54*, 547–560. [[CrossRef](#)]
13. Chu, J.; Yan, S. Estimation of degree of consolidation for vacuum preloading projects. *Int. J. Geomech.* **2005**, *5*, 158–165. [[CrossRef](#)]
14. Chai, J.; Miura, N.; Bergado, D.T. Preloading clayey deposit by vacuum pressure with cap-drain: Analyses versus performance. *Geotext. Geomembr.* **2008**, *26*, 220–230. [[CrossRef](#)]
15. Sun, L.; Guo, W.; Chu, J.; Nie, W.; Ren, Y.; Yan, S.; Hou, J. A pilot test on a membraneless vacuum preloading method. *Geotext. Geomembr.* **2017**, *45*, 142–148. [[CrossRef](#)]
16. Chai, J.; Rondonuwu, S.G. Surcharge loading rate for minimizing lateral displacement of PVD improved deposit with vacuum pressure. *Geotext. Geomembr.* **2015**, *43*, 558–566. [[CrossRef](#)]
17. Long, P.V.; Nguyen, L.V.; Bergado, D.T.; Balasubramaniam, A.S. Performance of PVD improved soft ground using vacuum consolidation methods with and without airtight membrane. *Geotext. Geomembr.* **2015**, *43*, 473–483. [[CrossRef](#)]
18. Lam, L.G.; Bergado, D.T.; Hino, T. PVD improvement of soft Bangkok clay with and without vacuum preloading using analytical and numerical analyses. *Geotext. Geomembr.* **2015**, *43*, 547–557. [[CrossRef](#)]
19. Zhang, Z.; Ye, G.B.; Xu, Y. Comparative analysis on performance of vertical drain improved clay deposit under vacuum or surcharge loading. *Geotext. Geomembr.* **2018**, *46*, 146–154. [[CrossRef](#)]
20. Ding, J.; Wan, X.; Zhang, C.; He, Z.; Zhao, L. Case Study: Ground Improvement of Yangtze River Floodplain Soils with Combined Vacuum and Surcharge Preloading Method. *Int. J. Geomech.* **2019**, *19*, 05019008.1–05019008.13. [[CrossRef](#)]
21. López-Acosta, N.; Espinosa-Santiago, A.L.; Pineda-Núñez, V.; Ossa, A.; Mendoza, M.J.; Ovando-Shelley, E.; Botero, E. Performance of a test embankment on very soft clayey soil improved with drain-to-drain vacuum preloading technology. *Geotext. Geomembr.* **2019**, *47*, 618–631. [[CrossRef](#)]
22. Yu, H.; Lu, C.; Chen, W.; Tian, H. An insight into the creep mechanisms of a clayey soil through long-term consolidation tests. *Bull. Eng. Geol. Environ.* **2021**, *80*, 9127–9139. [[CrossRef](#)]
23. Kumarage, P.I.; Gnanendran, C.T. Long-term performance predictions in ground improvements with vacuum assisted Prefabricated Vertical Drains. *Geotext. Geomembr.* **2019**, *47*, 95–103. [[CrossRef](#)]
24. Fellenius, B.H.; Harris, D.E.; Anderson, D.G. Static loading test on a 45 m long pipe pile in Sandpoint, Idaho. *Can. Geotech. J.* **2004**, *41*, 613–628. [[CrossRef](#)]
25. Lv, A.; Liang, J.; Zou, S.; Chen, X.; Li, Q. The device and experimental study of the monitoring of the layered soil settlement. *J. Phys. Conf. Ser.* **2021**, *1930*, 012017. [[CrossRef](#)]
26. Lei, H.; Feng, S.; Wang, L.; Jin, Y. Field instrumentation and settlement prediction of ground treated with straight-line vacuum preloading. *Geomech. Eng.* **2019**, *19*, 447–462.
27. Asaoka, A. Observational Procedure of Settlement Prediction. *Soils Found.* **1978**, *18*, 87–101. [[CrossRef](#)] [[PubMed](#)]
28. Chai, J.; Carter, J.; Hayashi, S. Ground deformation induced by vacuum consolidation. *J. Geotech. Geoenviron. Eng.* **2005**, *131*, 1552–1561. [[CrossRef](#)]
29. Xu, H.; Deng, X.J.; Qi, Y.Z. Development of shear strength of soft clay under vacuum preloading. *Chin. J. Geotech. Eng.* **2010**, *32*, 6. (In Chinese)

30. Mo, H.; Wang, J.; Lin, Y. Macro and micro analyses of effectiveness by vacuum preloading treatment of soft soil. *Chin. J. Rock Mech. Eng.* **2013**, *32*, 6. (In Chinese)
31. Bergado, D.T.; Balasubramaniam, A.; Fannin, R.J.; Holtz, R.D. Prefabricated vertical drains (PVDs) in soft Bangkok clay: A case study of the new Bangkok International Airport project. *Can. Geotech. J.* **2002**, *39*, 304–315. [[CrossRef](#)]
32. Long, P.V.; Bergado, D.T.; Giao, P.H.; Balasubramaniam, A.; Quang, N.C. Back analyses of compressibility and flow parameters of PVD improved soft ground in Southern Vietnam. In Proceedings of the 8th International Conference on Geosynthetics, Yokohama, Japan, 18–22 September 2006; pp. 465–468.
33. Chai, J.C.; Miura, N.; Nomura, T. Effect of hydraulic radius on long-term drainage capacity of geosynthetic drains. *Geotext. Geomembr.* **2004**, *22*, 3–16. [[CrossRef](#)]
34. Wang, P.; Wu, J.; Ge, X.; Chen, F.; Yang, X. Non-uniform Consolidation of Soil and Influence of Corresponding Clogging Effect During Vacuum Preloading. *Int. J. Geosynth. Ground Eng.* **2022**, *8*, 58. [[CrossRef](#)]
35. Mesri, G.; Khan, A.Q. Ground Improvement Using Vacuum Loading Together with Vertical Drains. *J. Geotech. Geoenviron. Eng.* **2012**, *138*, 680–689. [[CrossRef](#)]
36. Feng, S.; Bai, W.; Lei, H.; Song, X.; Liu, W.; Cheng, X. Vacuum preloading combined with surcharge preloading method for consolidation of clay-slurry ground: A case study. *Mar. Georesour. Geotechnol.* **2023**, 1–14. [[CrossRef](#)]
37. Wu, Y.; Jiang, H.; Lu, Y.; Sun, D. Experimental study on treatment of waste slurry by vacuum preloading with different conditioning agents. *Geomech. Eng.* **2019**, *17*, 543–551.
38. Lei, H.; Lu, H.; Liu, J.; Zheng, G. Experimental study of the clogging of dredger fills under vacuum preloading. *Int. J. Geomech.* **2017**, *17*, 04017117. [[CrossRef](#)]
39. Wang, Z.L.; Zheng, M.X.; Li, Y.C. Research on mathematic model method for calculating pre-consolidation pressure and its application. *Yantu Lixue/Rock Soil Mech.* **2005**, *27*, 1587–1590.

Disclaimer/Publisher's Note: The statements, opinions and data contained in all publications are solely those of the individual author(s) and contributor(s) and not of MDPI and/or the editor(s). MDPI and/or the editor(s) disclaim responsibility for any injury to people or property resulting from any ideas, methods, instructions or products referred to in the content.